

# Synthesis of p-Type Gallium Nitride Nanowires for Electronic and Photonic Nanodevices

Zhaohui Zhong,<sup>†,§</sup> Fang Qian,<sup>†,§</sup> Deli Wang,<sup>†,§</sup> and Charles M. Lieber<sup>\*,†,‡</sup>

*Department of Chemistry and Chemical Biology, Harvard University, 12 Oxford Street, Cambridge, Massachusetts 02138, and Division of Engineering and Applied Sciences, Harvard University, Cambridge, Massachusetts 02138*

*Received January 4, 2003; Revised Manuscript Received January 24, 2003*

## ABSTRACT

Magnesium-doped gallium nitride nanowires have been synthesized via metal-catalyzed chemical vapor deposition. Nanowires prepared on *c*-plane sapphire substrates were found to grow normal to the substrate, and transmission electron microscopy studies demonstrated that the nanowires had single-crystal structures with a  $\langle 0001 \rangle$  growth axis that is consistent with substrate epitaxy. Individual magnesium-doped gallium nitride nanowires configured as field-effect transistors exhibited systematic variations in two-terminal resistance as a function of magnesium dopant incorporation, and gate-dependent conductance measurements demonstrated that optimally doped nanowires were p-type with hole mobilities of ca.  $12 \text{ cm}^2/\text{V}\cdot\text{s}$ . In addition, transport studies of crossed gallium nitride nanowire structures assembled from p- and n-type materials show that these junctions correspond to well-defined p–n diodes. In forward bias, the p–n crossed nanowire junctions also function as nanoscale UV-blue light emitting diodes. The new synthesis of p-type gallium nitride nanowire building blocks opens up significant potential for the assembly of nanoscale electronics and photonics.

Semiconductor nanowires (NWs) have demonstrated significant potential as fundamental building blocks for nano-electronic and nanophotonic devices and also offer substantial promise for integrated nanosystems.<sup>1,2</sup> A key feature of semiconductor NWs that has enabled much of their success has been the growth of materials with reproducible electronic properties, including the controlled incorporation of n-type and/or p-type dopants.<sup>3–5</sup> The ability to incorporate both p- and n-type dopants in a single material system, called complementary doping, has been previously demonstrated in silicon (Si)<sup>3,4</sup> and indium phosphide (InP)<sup>5</sup> NWs and has opened up substantial opportunities for exploring nanodevice concepts. For example, p-type and n-type Si NWs have been used to assemble p–n diodes, bipolar transistors, and complementary inverters,<sup>3,4</sup> while p- and n-type InP NWs have been used to create p–n diodes that function as nanoscale near-infrared light-emitting diodes (LEDs).<sup>5</sup>

Complementary doping has not been reported in other semiconductor NW materials, although these previous results for Si and InP NWs underscore how the availability of p- and n-type materials can enable a wide-range of function. For example, there has been considerable interest in GaN NWs<sup>6–8</sup> since this wide band gap material has been used in

conventional planar structures to fabricate UV-blue LEDs and lasers,<sup>9</sup> as well as a range of other high-performance electronic devices.<sup>10</sup> Studies of the electronic properties of GaN NWs show, however, that unintentionally doped materials are intrinsically n-type,<sup>11,12</sup> and thus alone preclude exploration of a wide-range of nanodevices based upon complementary materials.

To overcome this limitation of available GaN NWs, we have previously used p-Si NWs and n-GaN NWs to assemble hetero p–n junctions and nano-LEDs,<sup>11,13</sup> although a limitation of using p-Si NWs in these nanostructures is that the band offsets yield a large asymmetry in the barriers for injection of holes and electrons at the junction. The synthesis of p-type GaN NWs could eliminate this issue and thus should impact further development of GaN NW-based electronics and photonics. Herein we report the first successful synthesis of p-type GaN (p-GaN) NWs, where magnesium is used as the p-type dopant,<sup>9</sup> and the assembly and characterization of p-GaN single NW field-effect transistors (FETs), p-GaN/n-GaN crossed NW diodes, and UV-blue p-GaN/n-GaN crossed NW nanoLEDs.

GaN NWs were prepared via metal-catalyzed chemical vapor deposition (CVD), using ammonia (99.99%, Matheson), gallium metal (99.9999%, Alfa Aesar), and magnesium nitride ( $\text{Mg}_3\text{N}_2$ , 99.6%, Alfa Aesar) as the N, Ga, and Mg sources, respectively, and *c*-plane sapphire as the growth substrate. The  $\text{Mg}_3\text{N}_2$  decomposes thermally as  $\text{Mg}_3\text{N}_2(\text{s}) =$

\* Corresponding author.

<sup>†</sup> Department of Chemistry and Chemical Biology.

<sup>‡</sup> Division of Engineering and Applied Sciences.

<sup>§</sup> These authors contributed equally to this work.

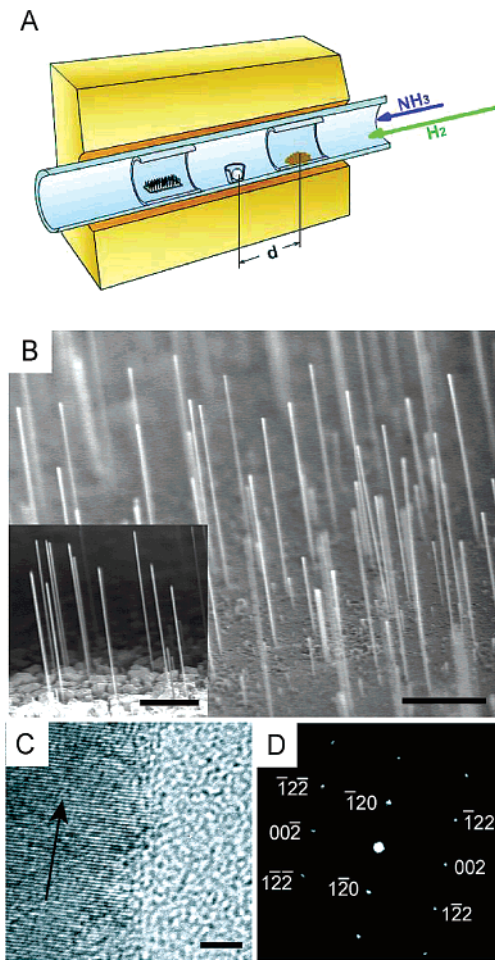


**Figure 1.** (A) Schematic of growth apparatus, where the separation between Ga and  $\text{Mg}_3\text{N}_2$  sources is  $d$ . The Ga source was fixed at a distance of 0.5 in. upstream from the substrate. (B) FE-SEM images of as grown GaN NWs on  $c$ -plane sapphire substrate. Scale bars are  $10\ \mu\text{m}$ . (C) Lattice-resolved TEM image of a single 20 nm diameter GaN NW. The black arrow highlights NW axis, which corresponds to the  $\langle 0001 \rangle$  direction; the scale bar is 5 nm. (D) Electron diffraction pattern recorded along the  $[10\bar{1}0]$  zone axis with  $(hkl)$  indices shown.

$3\text{Mg}(\text{g}) + \text{N}_2(\text{g})$  to yield Mg dopant and was located upstream of the Ga-source; the separation was systematically varied to control dopant incorporation (Figure 1A). Field-emission scanning electron microscopy (FE-SEM) images of GaN NWs prepared at  $950\ ^\circ\text{C}$  using nickel catalyst<sup>14</sup> show that essentially all of the GaN NWs grow normal to the sapphire surface with lengths from 10 to  $40\ \mu\text{m}$  (Figure 1B). This normal orientation observed for the NWs suggests that substrate-NW epitaxy may be important in defining the growth direction. Similar data were obtained when the Mg–Ga source separation was varied from 1 to 6 in.

Transmission electron microscopy (TEM) was used to further characterize the Mg-doped GaN NWs. Low-resolution images show that the NWs have diameters ranging from ca. 20 to 100 nm and, moreover, that the NW ends terminate in nanoscale Ni-based clusters similar in size to the NW diameters. These latter observations suggest strongly that NW growth proceeds via a nanocluster catalyzed vapor–liquid–solid mechanism.<sup>1,2</sup> Lattice-resolved images (Figure 1C) and

electron diffraction data (Figure 1D) further show that the Mg-doped GaN NWs are single-crystal materials with a  $\langle 0001 \rangle$  growth direction and lattice constants ( $a = 0.319$  and  $c = 0.517$  nm), in agreement with wurtzite GaN.<sup>15</sup> The GaN NW growth direction and orientation is consistent with epitaxial growth from the  $c$ -plane sapphire surface; this explanation agrees with results from previous thin film studies where GaN has been shown to grow epitaxially on  $c$ -plane sapphire.<sup>16</sup> In addition, energy-dispersive X-ray fluorescence (EDX) analysis of GaN NWs showed no Mg, although this is consistent with the instrument sensitivity (ca. 0.5 atomic %) and expected Mg doping levels ( $< 10^{20}$  atoms/ $\text{cm}^3 \approx 0.23$  atomic %). Clear evidence for incorporation of active Mg-dopants was obtained, however, from electrical transport measurements.

GaN NWs were configured as FETs to investigate the effects of growth parameters on Mg-doping.<sup>17</sup> First, we find that the two-terminal resistance varied systematically with the Ga–Mg source separation,  $d$  (Figure 2A). The initial decrease and subsequent increase in resistance with decreasing  $d$  is consistent with increasing Mg concentration since above an optimal doping level Mg self-compensation occurs.<sup>18,19</sup> Second, current ( $I$ ) versus source-drain voltage ( $V_{\text{sd}}$ ) and gate voltage ( $V_{\text{g}}$ ) were recorded to determine the sign of the carriers produced by the Mg dopant. The data exhibit a conductance increase (decrease) for  $V_{\text{g}}$  less (greater) than zero (Figure 2B) and thus demonstrate that the Mg-doped GaN NWs are p-type. Results from different samples further show that NWs prepared with Ga–Mg source separations from 1 to 4 in. are p-type, although larger values of  $d$ , which yield lower concentrations of Mg, lead to n-type materials. These observations are consistent with the significant n-type doping due to nitrogen vacancies and/or oxygen impurities in as-grown GaN NWs,<sup>11</sup> since these “intrinsic” dopants must be compensated (by Mg) before p-type behavior is observed.

In addition, we examined in more detail the transport characteristics of FETs based on optimally doped p-GaN NW (i.e., samples with minimum resistance at  $d = 3$  in.) to determine hole mobilities. A representative conductance versus  $V_{\text{g}}$  plot (Figure 2C) exhibits a relatively sharp onset, steep increase, and finally saturation in the conductance with decreasing  $V_{\text{g}}$ . The hole mobility estimated from these data is  $12\ \text{cm}^2/\text{V}\cdot\text{s}$ .<sup>20</sup> We believe that this value likely represents a lower bound on the possible mobility in p-GaN NWs (e.g., factors such as dopant activation, gate dielectric, and contact formation have not been optimized), although it is nevertheless comparable to the best values,  $10\ \text{cm}^2/\text{V}\cdot\text{s}$ , reported for planar p-GaN devices.<sup>21</sup>

Last, these new p-GaN NWs together with n-GaN materials have been exploited to assemble complementary crossed NW p–n structures (Figure 3A). Transport measurements made on crossed NW p–n junctions show well-defined current rectification that is characteristic of p–n diodes (Figure 3B). Specifically, little current is observed in reverse bias to  $V_{\text{sd}} \approx -5$  V, and there is a sharp current turn-on in forward bias at ca. 3.5 V. The  $I$ – $V$  data recorded from the individual p-GaN and n-GaN NWs were symmetric (inset,

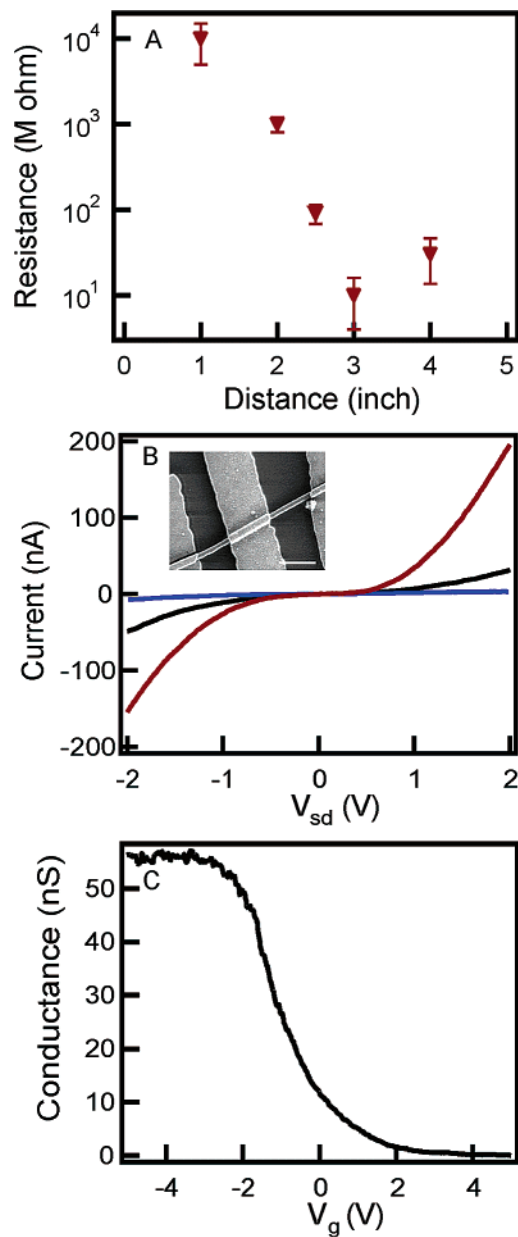


**Figure 2.** (A) Resistance of as grown p-GaN NWs versus  $d$ . (B)  $I$ - $V_{sd}$  data for a p-GaN NW prepared with  $d = 3$  in. The  $V_g$  are  $-2$  (red),  $0$  (black), and  $+2$  V (blue). (inset) FE-SEM image of a representative p-GaN NW device. Scale bar is  $1 \mu\text{m}$ . (C) Conductance versus  $V_g$  for the device shown in (B).

Figure 3B), and thus we can attribute the rectification to the crossed NW p-n junction and not to NW-metal contacts. In addition, the current turn-on at  $3.5$  V is consistent with the band-gap for GaN in this p-GaN/n-GaN device and contrasts the much lower current turn-on voltage for p-Si/n-GaN heterojunctions.<sup>11</sup>

Significantly, optical studies demonstrate that these crossed GaN NW p-n junctions exhibit UV-blue light emission in forward bias. Electroluminescence (EL) measurements on individual crossed GaN NW p-n diodes made using a home-built, far-field epifluorescence microscope show that emission is localized at the nanowire cross point and is thus consistent with EL from the forward biased p-n nanojunctions (inset, Figure 3C). EL spectra recorded from forward biased

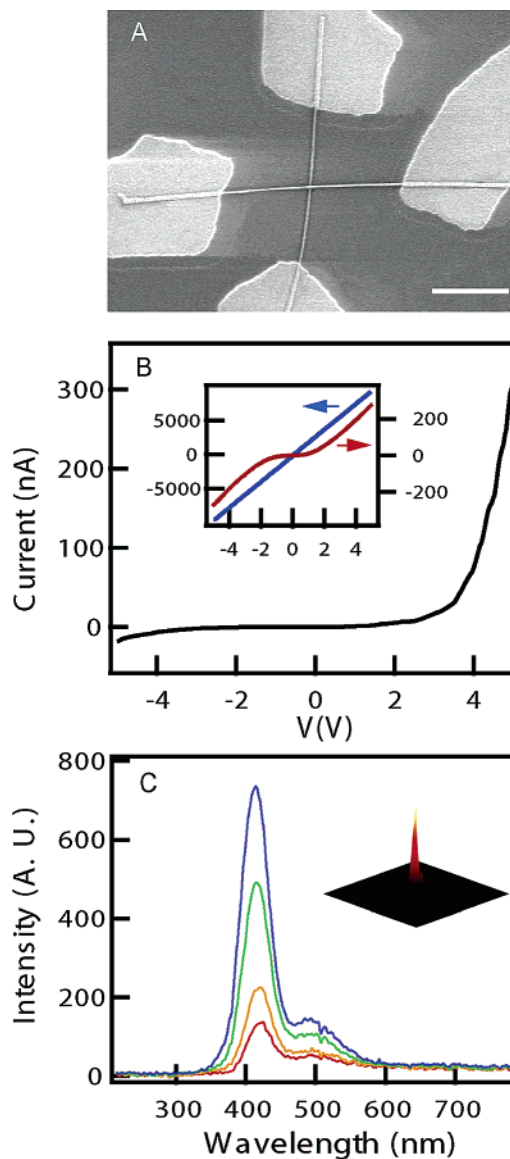


**Figure 3.** (A) FE-SEM image of a crossed GaN NW p-n device. Scale bar is  $2 \mu\text{m}$ . (B)  $I$ - $V$  data recorded for the p-GaN/n-GaN crossed NW junction. (inset)  $I$ - $V$  data for the n-GaN NW (blue) and the p-GaN NW (red). (B) EL spectra recorded from a p-GaN/n-GaN crossed NW junction in forward bias. The red, yellow, green, and blue EL spectra were recorded with injection currents of  $61$ ,  $132$ ,  $224$ , and  $344$  nA, respectively. (inset) Image of the emission from the crossed NW junction.

nanoscale p-n junction exhibit a dominant emission peak centered at  $415$  nm and a smaller peak at ca.  $493$  nm (Figure 3C). Previous studies of planar LEDs suggest that the  $415$  nm EL peak can be attributed to radiative recombination from the conduction band to deep levels associated with the Mg dopants,<sup>22</sup> while the  $493$  nm peak is due to recombination from other impurity levels. We also find that at higher injection currents the p-n diodes exhibit UV band-edge emission at ca.  $380$  nm that is similar to strongly driven planar GaN LEDs.<sup>9</sup> Future investigations of individual p- and n-GaN NWs and crossed NW junction properties should enable further improvements in these UV nanoscale LEDs, although we believe that these nanodevices represent unique photonic sources even in their present form.

In summary, p-type single-crystal GaN NWs have been synthesized via metal-catalyzed chemical vapor deposition using Mg as the dopant. NWs prepared on *c*-plane sapphire substrates grow epitaxially with a  $\langle 0001 \rangle$  growth direction. Gate-voltage dependent studies of individual Mg-doped GaN NWs configured as field-effect transistors (FETs) demonstrated unambiguously that the NWs are p-type with maximum hole mobilities of ca.  $12 \text{ cm}^2/\text{V}\cdot\text{s}$ . In addition, transport studies of crossed GaN NW structures assembled from p- and n-type materials show that the nanoscale junctions behave as well-defined p–n diodes, and significantly, these p–n crossed NW junctions function as nanoscale UV-blue LEDs. We believe that the realization of p-type doping in GaN NWs opens up significant potential for the assembly of nanoscale electronics and photonics.

**Acknowledgment.** We thank L. Z. Yuan and C. Y. Wen for assistance with TEM measurements. C.M.L. acknowledges the Air Force Office of Scientific Research for generous support of this work.

## References

- (1) Lieber, C. M. *Sci. Am.* September, **2001**, 58.
- (2) Hu, J.; Odom, T. W.; Lieber, C. M. *Acc. Chem. Res.* **1999**, 32, 435.
- (3) Cui, Y.; Lieber, C. M. *Science* **2000**, 291, 891.
- (4) Cui, Y.; Duan, X.; Hu, J.; Lieber, C. M.; *J. Phys. Chem. B* **2000**, 104, 5213.
- (5) Duan, X.; Huang, Y.; Cui, Y.; Wang, J.; Lieber, C. M. *Nature* **2001**, 409, 66.
- (6) Duan, X.; Lieber, C. M. *J. Am. Chem. Soc.* **2000**, 122, 188.
- (7) Chen, C.; Yeh, C.; Chen, C.; Yu, M.; Liu, H.; Wu, J.; Chen, K.; Chen, L.; Peng, J.; Chen, Y. *J. Am. Chem. Soc.* **2001**, 123, 2791.
- (8) Johnson, J. C.; Choi, H.; Knutsen, K. P.; Schaller, R. D.; Yang, P.; Saykally, R. J. *Nature Mater.* **2002**, 1, 106.
- (9) Nakamura, S.; Fasol, G. *The Blue Laser Diode: GaN Based Light Emitters and Lasers*; Springer-Verlag: New York, 1997.
- (10) Pearton, S. J.; Ren, F. *Adv. Mater.* **2000**, 12, 1571.
- (11) Yu, H.; Duan, X.; Cui, Y.; Lieber, C. M. *Nano Lett.* **2002**, 2, 101.
- (12) Kim, J.; So, H.; Park J.; Kim, J.; Kim, J.; Lee, C.; Lyu, S. *Appl. Phys. Lett.* **2002**, 80, 3548.
- (13) Huang, Y.; Duan, X.; Lieber, C. M., submitted for publication.
- (14) A drop of 0.02 M ethanol solution of  $\text{Ni}(\text{NO}_3)_2$  was deposited on the substrate, and then the growth was carried out at  $950 \text{ }^\circ\text{C}$  using 30 sccm (standard cubic centimeter per minute)  $\text{NH}_3$  and 60 sccm  $\text{H}_2$  at 200 Torr for 20 min.
- (15) Zhu, Q.; Botchkarev, A.; Kim, W.; Aktas, Ö.; Salvador, A.; Sverdlov, B.; Morkoc, H.; Tsen, S.-C. Y.; Smith, D. J. *Appl. Phys. Lett.* **1996**, 68, 1141.
- (16) Liu, L.; Edgar, J. H. *Mater. Sci. Eng. R* **2002**, 37, 61.
- (17) As grown GaN NWs were annealed at  $900 \text{ }^\circ\text{C}$  for 10 min under nitrogen<sup>9</sup> to activate the Mg dopant. Annealed GaN NWs in ethanol were dispersed on substrates and FET devices were defined by electron beam lithography as described previously.<sup>3,4</sup> Source-drain electrodes were deposited by thermal evaporation of Ni/Au (50/70 nm) and annealed at  $450 \text{ }^\circ\text{C}$  for 3 min in  $\text{O}_2$  flow.<sup>23</sup> The top-gate was prepared in a separate step by deposition of  $\text{Al}_2\text{O}_3/\text{Au}$  (30/100 nm).
- (18) Obloh, H.; Bachem, K. H.; Kaufmann, U.; Kunzer, M.; Maier, M.; Ramakrishnan, A. *J. Cryst. Growth* **1998**, 195, 270.
- (19) There are two contributions to the observed results. First, under the low flow rates (30 sccm  $\text{NH}_3$  and 60 sccm  $\text{H}_2$ ) there is reaction of the dopant source and dopant with the reactor wall. This reaction depletes the Mg dopant increasingly with distance under isothermal conditions. Second, there is a small temperature gradient in the reactor (dropping  $5 \text{ }^\circ\text{C}$  at 3 in., and  $25 \text{ }^\circ\text{C}$  at 5 in.) that can reduce the dopant vapor pressure. Previous studies show that the equilibrium constant for decomposition of  $\text{Mg}_3\text{N}_2$  decreases by 1 order of magnitude for a  $25 \text{ }^\circ\text{C}$  drop in temperature (Soulen, J. R.; Sthapitanonda, P.; Margrave, J. L. *J. Phys. Chem.* **1955**, 59, 132), although this drop only produces a relatively small change in Mg concentration.
- (20) Cui, Y.; Zhong, Z.; Wang, D.; Wang, W. U.; Lieber, C. M. *Nano Lett.* **2003**, 3, 149.
- (21) Keller, S.; DenBaars, S. P. *J. Cryst. Growth* **2003**, 248, 479.
- (22) Smith, M.; Chen, G.; Lin, J.; Jiang, H.; Salvador, A.; Sverdlov, B. N.; Morkoc, H.; Goldenberg, B. *Appl. Phys. Lett.* **1996**, 68, 1883.
- (23) Zhang, A. P.; Lou, B.; Johnson, J. W.; Ren, F. *Appl. Phys. Lett.* **2001**, 79, 3636.

NL034003W